

# 16-channel tunable and 25-Gb/s EAM-integrated DBR-LD for WDM-based mobile front-haul networks

OH KEE KWON,\* CHUL WOOK LEE, SU HWAN OH, AND KI SOO KIM

*Photonics Convergence Components Research Group, Electronics and Telecommunications Research Institute, 218 Gajeongno, Yuseong-gu, Daejeon, Republic of Korea*

\*okkwon@etri.re.kr

**Abstract:** We report a tunable distributed Bragg reflector-laser diode (DBR-LD) integrated with an electro-absorption-modulator (EAM) at an operating wavelength of 1.3  $\mu\text{m}$ . This LD consists of gain, phase control (PC), DBR, and EAM sections, realized by using a butt-coupling technique in monolithically integrating the multiple quantum wells (MQWs) with the passive core and by applying an etched-mesa buried hetero-structure (EMBH) to the resonance cavity (i.e., gain to DBR section) and a deep-ridge type to the EAM section in fabricating the waveguide structure. Wavelength tuning of the LD is achieved by both applying a voltage to the heater metal of DBR section (coarse tuning) and injecting a current to the ohmic metal of PC section (fine tuning). From the work, the fabricated chips show a threshold current of about 13 mA, a side mode suppression ratio (SMSR) of more than 35 dB, and a tuning range of 15 nm within a heater voltage of 2 V. Dynamic tests for the EAM-integrated LD show the 3 dB bandwidth of more than 20 GHz and clear 25 Gb/s eye openings with a dynamic extinction ratio (DER) of over 7 dB for 16 channels spaced at the wavelength interval of 0.55 nm. Based on these results, we conclude that the EAM-integrated DBR-LD is capable of providing 16 channel operation at a data rate of 25 Gb/s and can be used as an effective light source for WDM-based mobile front-haul networks.

© 2021 Optical Society of America under the terms of the [OSA Open Access Publishing Agreement](#)

## 1. Introduction

Wavelength-tunable lasers are required for a wide variety of wavelength division multiplexed (WDM) systems, packet switching (PS) architectures, reconfigurable optical add/drop multiplexed (ROADM) systems, and software defined networks (SDNs), since they realize effectively employing wavelength resources, dynamic wavelength provisioning, and flexible network [1,2]. In particular, they have also attracted considerable interests in a mobile front-haul network for the purpose of inventory cost reduction and auxiliary management & channel control (AMCC) [3,4]. These LDs in this network must tune across a substantial number of channels while satisfying requirements in each channel, and also be cost-effective and provide similar operational performance as wavelength-fixed counterparts.

A distributed Bragg reflector-laser diode (DBR-LD) with a single grating mirror is one of the most suitable candidates owing to its compact size, easy fabrication, and simple wavelength calibration, compared with other types of DBR structures [5–7]. Although many studies have been conducted to realize this type of tunable laser [8–12], with the exception of Ref. [8], most of them have focused on the LDs operating at the C-band for dense DWDM applications (i.e., Recommendation ITU-T G.694.1) and for a wider wavelength tuning range (instead of using the O-band) as explained in Ref. [7].

Recently, we developed the O-band DBR-LD within the 15 nm tuning range only using heater tuning method and demonstrated 16 channel and 10 Gb/s operation under the direct modulation, where the extinction ratio (ER) of over 5.4 dB was shown for all channels [13]. From this result, we think the directly modulated DBR-LD using heater tuning method can be effectively utilized

as a low-cost light source enabling the common public radio interface (CPRI) line bit rate option 7/8/9 in the mobile front-haul network based on the multichannel CWDM applications with multi sub-channel optical interface [14,15].

To extent this line bit rate to option 10, it is required to develop the O-band tunable LD operating at bit rate of 25 Gb/s. In this paper, we fabricate a DBR-LD integrated with an electro-absorption-modulator (EAM) where the continuous wave (CW) light generated by the resonance cavity is intensity-modulated by the temporal change of the optical absorption, and demonstrate 25 Gb/s modulation for 16 channels.

The rest of this paper is organized as follows. In section 2, the design and fabrication of the EAM-integrated DBR-LD are described. In section 3, the experimental results of the fabricated LDs are shown and discussed. Finally, section 4 summarizes the results of this work.

## 2. Design and fabrication

A schematic chip diagram (top-view) and the epitaxial layer structure (side-view) of the EAM-integrated DBR-LD are depicted in Figs. 1(a) and 1(b), respectively. This LD has five sections; EAM, passive waveguide (WG), DBR, phase control (PC), and gain (from left to right). The length of each section was designed to be 180  $\mu\text{m}$ , 320  $\mu\text{m}$ , 230  $\mu\text{m}$ , 50  $\mu\text{m}$  and 350  $\mu\text{m}$ , respectively. The output light is emitted from the facet of EAM, and is modulated by the voltage  $V_{\text{EAM}}$  through the ohmic metal of EAM section. The output wavelength is determined by lasing condition of the resonator of which the cavity is formed from the DBR to the gain section, and is tuned coarsely by the voltage  $V_{\text{heat}}$  applied to the heater implemented on the waveguide of DBR section and tuned fine by the current  $I_{\text{PC}}$  through the ohmic metal of PC section [13]. For this structure,

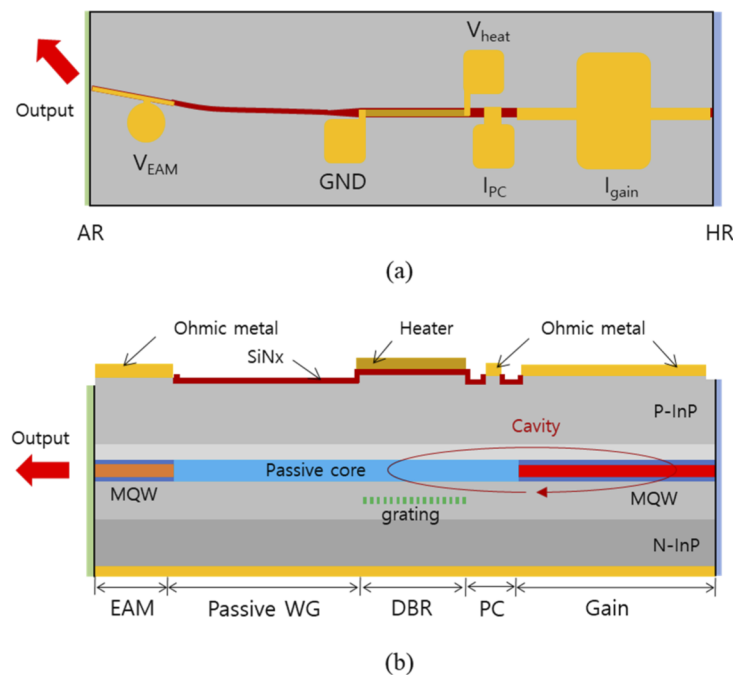


**Fig. 1.** (a) Schematic diagram and (b) layer structure of the EAM-integrated DBR-LD. The facets are anti-reflection (AR) and high reflection (HR)-coated.  $I_{\text{gain}}$  and  $I_{\text{PC}}$  denote the currents for the gain and PC sections.  $V_{\text{heat}}$  and  $V_{\text{EAM}}$  are the voltages for the DBR (heater) and EAM (ohmic metal), respectively.

the output facet is anti-reflection (AR)-coated and its waveguide is 9 degree-tilted to reduce the residual optical feedback from the output facet [16].

The InGaAsP/InP-based epitaxial layers were grown using metal-organic chemical vapor deposition (MOCVD). During the monolithic integration between two multiple-quantum-wells (MQWs) and passive core, two-time butt-joint coupling method (i.e. the first MQW-MQW integration and the second MQWs-passive core integration) was used. For those epitaxial structures, the MQW of the gain section was designed to generate an optical gain near the wavelength of 1.3  $\mu\text{m}$  and that of the EAM to have the wavelength detuning of about 50 nm from the lasing wavelength of DBR-LD. Specifically, the MQW of the gain section contains seven 6nm-thick InGaAsP (bandgap wavelength  $\lambda_g \cong 1.38 \mu\text{m}$ , compressive 0.8%) wells and eight 8nm-thick InGaAsP ( $\lambda_g \cong 1.1 \mu\text{m}$ , tensile 0.6%) barriers, and two SCH layers with a 35nm-thick InGaAsP ( $\lambda_g \cong 1.08 \mu\text{m}$ ) and a 45nm-thick InGaAsP ( $\lambda_g \cong 1.05 \mu\text{m}$ ). The MQW of the EAM section contains ten 8.5nm-thick InGaAsP ( $\lambda_g \cong 1.28 \mu\text{m}$ , compressive 0.5%) wells and eleven 6nm-thick InGaAsP ( $\lambda_g \cong 1.1 \mu\text{m}$ , tensile 0.4%) barriers, and a SCH layer with a 70 nm-thick InGaAsP ( $\lambda_g \cong 1.15 \mu\text{m}$ ). The passive core and grating layers have a 0.27- $\mu\text{m}$  thick InGaAsP ( $\lambda_g \cong 1.15 \mu\text{m}$ ) and a 25-nm thick InGaAsP ( $\lambda_g \cong 1.2 \mu\text{m}$ ), respectively. In order to increase the output power efficiency for this structure, it is desirable for the reflectivity of grating to be designed to have a smaller value than that of high reflection (HR)-facet. Taking this into account, and the period and duty cycle of the grating were designed to satisfy the conditions for a lasing wavelength of near 1.3  $\mu\text{m}$  and a coupling coefficient of about 25  $\text{cm}^{-1}$ , respectively. After the growing processes, room-temperature photo-luminescent (PL) measurements were performed on the grown area of each section. Figure 2 shows the PL spectra of MQWs in the gain (black) and EAM (red) sections, and passive core (blue). The peak wavelengths in gain, EAM, and passive core are shown to be about 1.32 $\mu\text{m}$ , 1.25  $\mu\text{m}$ , and 1.15 $\mu\text{m}$ , respectively.

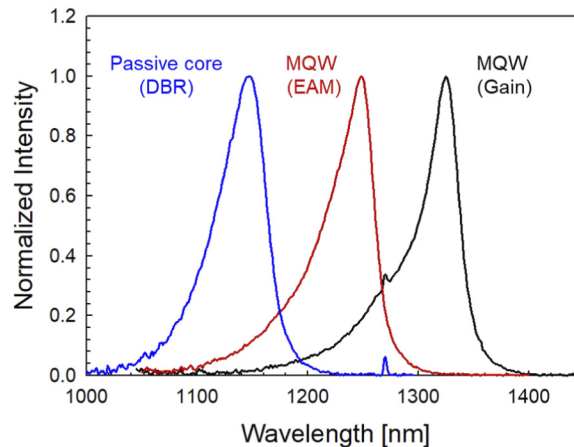


**Fig. 2.** PL spectra of MQWs in the gain (black) and EAM (red) sections, and passive core in DBR section (blue).

As for the waveguide structure, the resonant cavity (including the gain, PC, and DBR sections) was fabricated to be an etched-mesa buried hetero-structure (EMBH) for achieving a lower threshold current and a higher power efficiency [13,17], and the passive WG and EAM were fabricated to be a deep ridge waveguide (DRWG) for obtaining a lower bending loss and a lower parasitic capacitance, and the waveguide in the transition region between them was implemented to have low mode-transition loss using tapered structures in some part of passive WG section. After the fabrication of waveguide, benzo-cyclobutene (BCB) process was conducted and then a Ti/Pt/Au electrode was formed as p-type ohmic contact of the gain and EAM sections, and a

Cr/Au electrode was used as the heater metal of DBR section. The width and length of heater metal were designed to be  $6\ \mu\text{m}$  and  $200\ \mu\text{m}$ , respectively. On the bottom of wafer, a Cr/Au electrode was formed as n-type ohmic contact. To examine the operational properties of the fabricated LD, the chip was bonded onto a sub-mount with the electrical lines for light generation (Gain), wavelength tuning (PC and DBR), and modulation (EAM), and  $50\ \Omega$  load, as shown in Fig. 3.

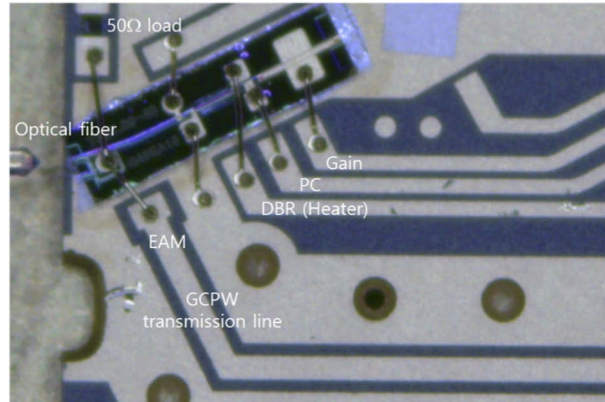


**Fig. 3.** A photograph on the EAM-integrated DBR-LD chip on the sub-mount with electrical lines and  $50\ \Omega$  load impedance. GCPW denoted grounded coplanar waveguide

### 3. Result and discussion

Figure 4(a) shows typical light versus gain current and applied voltage (L-I-V) characteristics of the fabricated LDs at an operating temperature of  $25^\circ\text{C}$ . It appears that the threshold current is within the range of  $13 \pm 1\ \text{mA}$ , the slope efficiency is about  $0.22\ \text{W/A}$ , and the output power is higher than  $25\ \text{mW}$  at the current of  $150\ \text{mA}$ . In the L-I curves, there is no kink which results from the longitudinal mode-hopping within this current range. Figure 4(b) shows the output spectrum

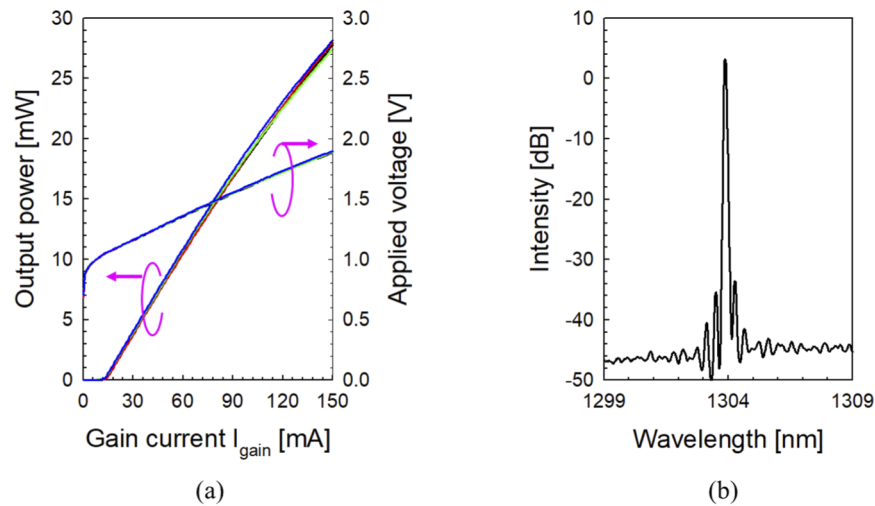


**Fig. 4.** (a) L-I-V characteristics of the fabricated EAM-integrated DBR-LDs and (b) output spectrum at the gain current of  $80\ \text{mA}$

spectrum at the current of 80 mA, and its peak wavelength  $\lambda_{\text{peak}}$  and side mode suppression ratio (SMSR) were obtained to be about 1304 nm and higher than 35 dB, respectively.

To examine the tuning properties of the DBR section, the  $\lambda_{\text{peak}}$  and the SMSR are tested as a function of the heater voltage  $V_{\text{heat}}$  as shown in Fig. 5. As the  $V_{\text{heat}}$  increases, the  $\lambda_{\text{peak}}$  moves toward a longer wavelength side due to the heat-induced refractive index change, and is changed with quadratic shape according to the linear relation between the thermal tuning and electrical power [12]. In this test, the  $\lambda_{\text{peak}}$  is tuned 1304 to 1319 nm and the SMSR is higher than 35 dB for the whole tuning range, and as a result, the tuning range of about 15 nm under the stable single mode operation is achieved within the  $V_{\text{heat}}$  of 2 V.

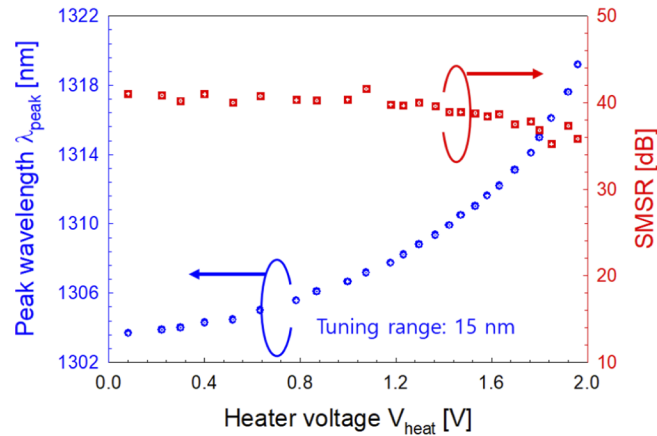


**Fig. 5.** Peak wavelength  $\lambda_{\text{peak}}$  (left-axis) and SMSR (right-axis) with respect to the heater voltage of DBR section  $V_{\text{heat}}$ . In this test, the gain current  $I_{\text{gain}}$  was fixed at 65 mA.

In order to examine the extinction properties of the EAM section, the output power is measured with the voltage applied to the EAM section  $V_{\text{EAM}}$  for different lasing wavelengths. Figure 6 shows the output power variation as a function of  $V_{\text{EAM}}$  for the lasing wavelengths of 1304, 1308, 1312 nm, respectively. In this measurement, all the measured powers were normalized by the

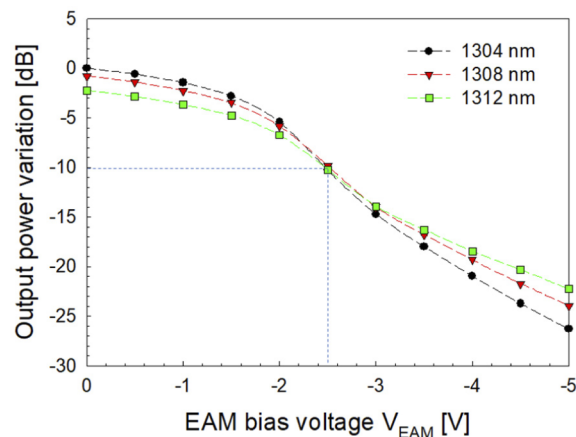


**Fig. 6.** Output power variation with respect to the bias voltage applied to the EAM  $V_{\text{EAM}}$  for the lasing wavelengths of 1304, 1308, and 1312 nm. In this figure, the power variations at the  $V_{\text{EAM}}$  of  $-2.5$  V are about  $-10$  dB for all wavelengths.

reference power measured at zero bias voltage for the wavelength of 1304 nm. It is clearly shown that, as the  $V_{EAM}$  increases, the output power is reduced with the reverse sigmoid-shape [18] and as the  $\lambda_{peak}$  moves to the longer wavelength side, the extinction ratio tends to be degraded gradually.

The electro-optic (EO) responses of the EAM-integrated DBR-LD are tested for various values of  $V_{EAM}$  as shown in Fig. 7, and the  $-3$  dB bandwidth appears to be about 20 GHz even at zero bias voltage. With this LD, the large-signal modulation was performed for 25 Gb/s with a pseudo random bit sequence (PRBS) of  $2^{31}-1$ . In this test,  $I_{gain}$ ,  $V_{EAM}$ , and the peak-to-peak voltage  $V_{pp}$  were fixed to be 65 mA,  $-2.2$  V and 2.5 V, respectively. Figure 8 and Fig. 9 show superimposed spectra of 16 channels spaced at the wavelength interval of 0.55 nm (which corresponds to 100 GHz at the wavelength of  $1.29\mu\text{m}$ ) and the corresponding eye diagrams, respectively. The spectra were obtained with a simultaneous control of the heater voltage of DBR section and the current of PC section (i.e., phase current). The phase current allowed all 16 channels to be aligned precisely at the interval of 0.55 nm, as shown in the peak wavelength difference of Fig. 10, with the SMSR of more than 35 dB even under the modulation. As for the 25 Gb/s eye

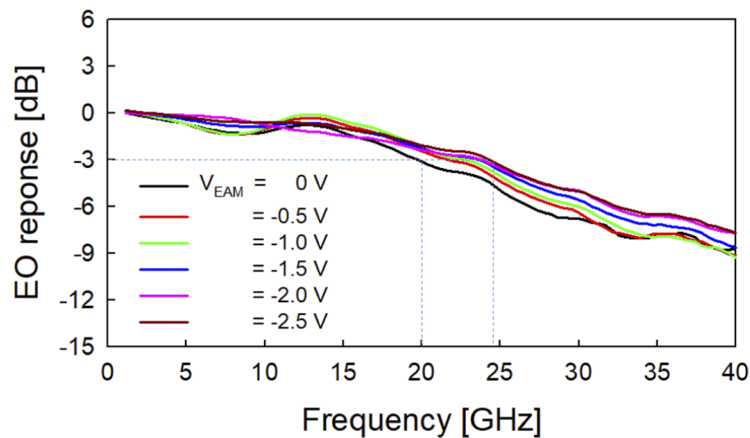


**Fig. 7.** EO responses for the EAM-integrated DBR-LD with respect to the  $V_{EAM}$ .  $-3$  dB modulation bandwidth is shown to be more than 20 GHz within the  $V_{EAM}$  of  $-2.5$  V.

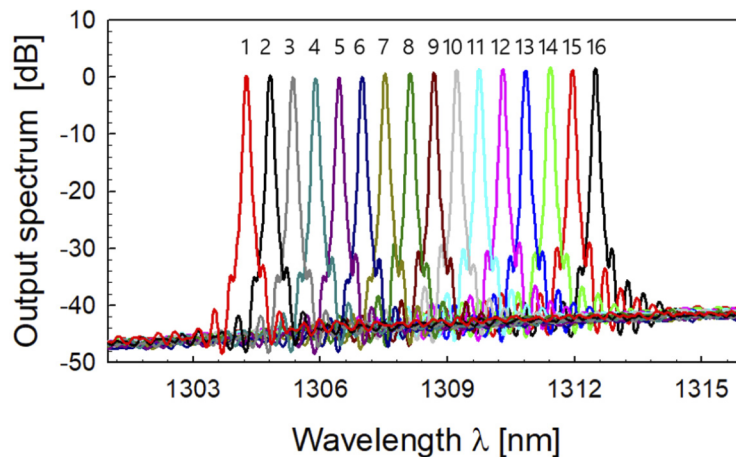


**Fig. 8.** A fiber coupled output spectra of 16 channel with a 0.55 nm spacing (i.e., 1304 to 1312.25 nm) under the 25 Gb/s modulation.

diagrams, the eye patterns are clearly opened with dynamic extinctions (DERs) of more than 7 dB (8.1 to 7.2 dB) for all channels as shown in Fig. 10. From these results, we confirm that the fabricated EAM-integrated DBR-LD is successfully operating over 25 Gb/s.

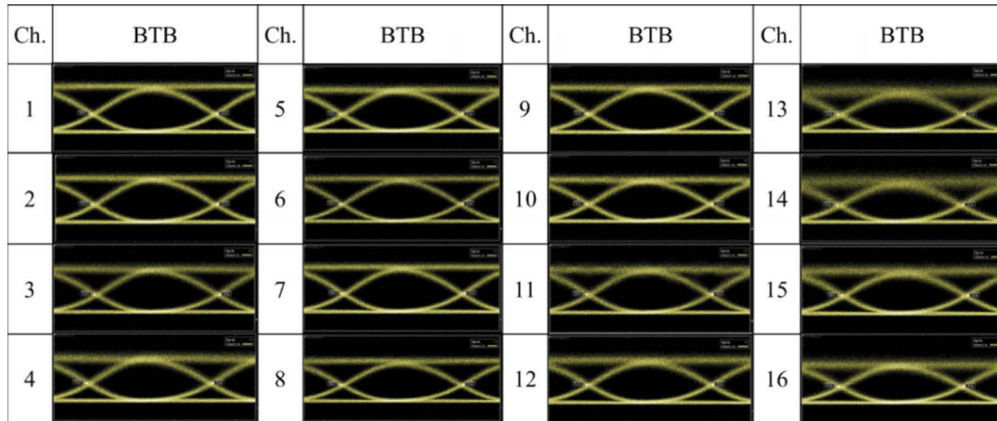


**Fig. 9.** Measured 25 Gb/s eye diagrams for 16 channels.

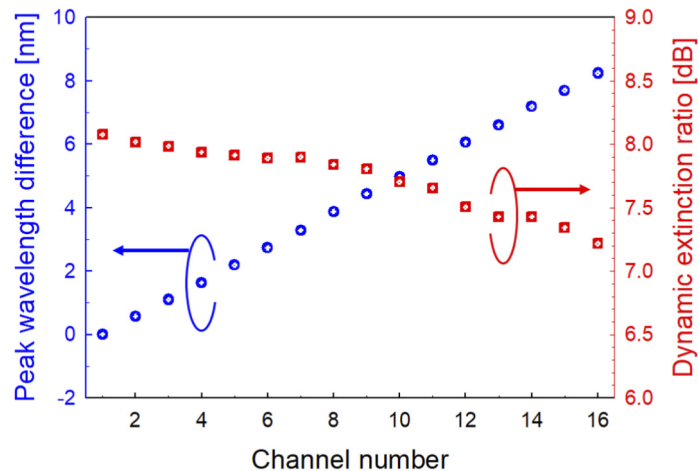


**Fig. 10.** Dynamic extinction ratio and peak wavelength difference with respect to channel number

#### 4. Summary

We developed an O-band tunable DBR-LD integrated with an EAM capable of supporting a 15 nm tuning range and 25 Gb/s modulation per channel. A 16 channels spaced at the wavelength grid of 0.55 nm with the SMSR of more than 35 dB were obtained by using a simultaneous control of the heater current and the phase current. In this integrated LD, the DBR-LD was fabricated using an EMBH for a low operating current and high output efficiency and the EAM was fabricated using the DRWG with BCB islands for a 25-Gb/s direct modulation. The threshold currents and  $-3$  dB BW of the fabricated LDs were about 13 mA and more than 20 GHz, respectively. The device shows clear eye patterns at BTB with a DER of over 7 dB at a  $V_{pp}$  of 2.5 V for all tuning

range. These results confirm that the EAM-integrated DBR-LD is useful for the 25 Gb/s direct modulation devices.

**Funding.** Ministry of Science and ICT, South Korea (2020-0-00847, 2020-0-01005).

**Disclosures.** The authors declare that there are no conflicts of interest related to this article.

## References

1. J. Zhu, A. Wonfor, S. H. Lee, S. Pachnicke, M. Lawin, R. V. Penty, J.-P. Elbers, R. Cush, M. J. Wale, and I. H. White, "Athermal colorless C-band optical transmitter system for passive optical networks," *J. Lightwave Technol.* **32**(22), 4253–4260 (2014).
2. A. Pizzinat, P. Chanclou, F. Saliou, and T. Diallo, "Things you should know about fronthaul," *J. Lightwave Technol.* **33**(5), 1077–1083 (2015).
3. I. A. Alimi, A. L. Teixeira, and P. P. Monterio, "Toward an efficient C-RAN optical fronthaul for the future networks: a tutorial on technologies requirements, challenges, and solutions," *IEEE Comm. Surveys & Tutorials* **20**(1), 708–769 (2018).
4. K. Honda, H. Nakamura, K. Hara, K. Sone, G. Nakagawa, Y. Hirose, T. Hoshida, and J. Terada, "Wavelength control method of upstream signals using AMCC in WDM-PON for 5G mobile fronthaul," *Opt. Express* **27**(19), 26749–26756 (2019).
5. H. Oh, H. Ko, K. S. Kim, J. M. Lee, C. W. Lee, O. K. Kwon, S. Park, and M. H. Park, "Fabrication of Butt-coupled SGDBR laser integrated with semiconductor optical amplifier having a lateral tapered waveguide," *ETRI J.* **27**(5), 551–556 (2005).
6. A. J. Ward, D. J. Robbins, G. Busico, E. Barton, L. Ponnampalam, J. P. Duck, N. D. Whitbread, P. Williams, D. C. J. Reid, A. C. Carter, and M. J. Wale, "Widely tunable DS-DBR laser with monolithically integrated SOA: Design and performance," *IEEE J. Sel. Top. Quantum Electron.* **11**(1), 149–156 (2005).
7. T. Shindo, N. Fujiwara, Y. Ohiso, T. Sato, and H. Matsuzaki, "Demonstration of 1.3 $\mu$ m wavelength range super structure grating DBR laser width wide wavelength tuning range of over 30 nm by introducing carrier confinement layers," *Proc. SPIE* **11301**, S01–S08 (2020).
8. M. Yamaguchi, M. Kitamura, S. Murata, I. Mito, and K. Kobayashi, "Wide range wavelength tuning in 1.3 (m) DBR-DC-PBH-LDs by current injection into the DBR region," *Electron. Lett.* **21**(2), 63–65 (1985).
9. T. L. Koch, U. Koren, and B. I. Miller, "High performance tunable 1.5 (m) InGaAs/InGaAsP multiple quantum well distributed Bragg reflector lasers," *Appl. Phys. Lett.* **53**(12), 1036–1038 (1988).
10. L. Han, S. Liang, H. Wang, L. Qiao, J. Xu, L. Zhao, H. Zhu, B. Wang, and W. Wang, "Electroabsorption-modulated widely tunable DBR laser transmitter for WDM-PONs," *Opt. Express* **22**(24), 30368–30376 (2014).
11. D. Zhou, S. Liang, L. Zhao, H. Zhu, and W. Wang, "High-speed directly modulated widely tunable two-section InGaAlAs DBR lasers," *Opt. Express* **25**(3), 2341–2346 (2017).
12. O. K. Kwon, C. W. Lee, K. S. Kim, S. H. Oh, and Y. A. Leem, "Proposal of novel structure for wide wavelength tuning in distributed Bragg reflector laser diode with single grating mirror," *Opt. Express* **26**(22), 28704–28712 (2018).
13. S. H. Oh, O. K. Kwon, K. S. Kim, and C. W. Lee, "1.3- (m) and 10-Gb/s tunable DBR-LD for low-cost application of WDM-based mobile front haul networks," *Opt. Express* **27**(20), 29241–29247 (2019).
14. J. Shin, S. Hong, J. Y. Lim, S. Cho, H. Y. Rhy, and G. Y. Yi, "CWDM network with dual sub-channel interface for mobile fronthaul and backhaul deployment," in *Proc. 16th Int. Conf. Adv. Commun. Technol. paper*, pp. 1009–1102 (2014).
15. TTA Standard for Multichannel CWDM Applications with Multi Sub-channel Optical Interface, TTAE.KO-03.0022/R2, 2018.
16. O. K. Kwon, Y. S. Baek, and Y. C. Chung, "Electroabsorption modulated laser with high immunity to residual facet reflection," *IEEE J. Quantum Electron.* **48**(9), 1203–1213 (2012).
17. O. K. Kwon, C. W. Lee, Y. A. Leem, K. S. Kim, S. H. Oh, and E. S. Nam, "1.5- (m) and 10 Gb/s etched mesa buried hetero-structure DFB-LD for datacenter networks," *Semicond. Sci. Technol.* **30**(10), 105010 (2015).
18. J. Shim, B. Liu, and J. E. Bowers, "Dependence of transmission curves on input optical power in an electroabsorption modulator," *IEEE J. Quantum Electron.* **40**(11), 1622–1628 (2004).